

RETRIEVAL OF VEGETATION WATER CONTENT USING BRIGHTNESS TEMPERATURES FROM THE SOIL MOISTURE ACTIVE PASSIVE (SMAP) MISSION

Steven K. Chan¹ and Rajat Bindlish²

¹ NASA Jet Propulsion Laboratory, California Institute of Technology, Pasadena, CA, USA

² NASA Goddard Space Flight Center, Greenbelt, MD, USA

ABSTRACT

In this paper, we explore a time series approach to using the tau-omega (τ - ω) model to retrieve vegetation water content (kg/m^2) with minimal use of ancillary data. Analytically, this approach calls for nonlinear optimization in two steps. First, multiple days of co-located brightness temperature observations are used to retrieve the effective vegetation opacity, which incorporates the combined radiometric and polarization effects of surface roughness and vegetation opacity. The resulting effective vegetation opacity is then used to retrieve vegetation water content to within a gain factor α and an offset factor β . By using a climatological vegetation water content ancillary database as the one adopted in the development of the SMAP standard and enhanced soil moisture products, α and β can be determined globally using the annual minimum and annual maximum of vegetation water content. The resulting values of α and β can then be used to reconstruct the retrieved vegetation water content. Formulation, assumptions, and limitations of this approach are presented alongside the preliminary global retrieval of vegetation water content using one year (2016) of SMAP brightness temperature observations.

Index Terms — SMAP, radiative transfer, vegetation, biomass, optimization.

1. INTRODUCTION

In passive remote sensing of soil moisture, vegetation is often a confounding factor to be corrected for in soil moisture estimation. This is especially true in soil moisture retrieval using a single polarized brightness temperature (T_B) channel [1], where accurate soil moisture retrieval hinges on accurate correction for the radiometric effects of vegetation and other parameters. In applications where the horizontally and vertically polarized T_B channels are used simultaneously in geophysical inversion, it is often possible to retrieve soil moisture as well as vegetation opacity (τ) [2]. While τ is directly proportional to vegetation water content (VWC), it is less relatable to practical field validation efforts because it is inherently a microwave attenuation property that depends on frequency and vegetation structure. Validation of τ would require elaborate and costly setup and maintenance of

antennas and their calibration. At spatial scales in typical satellite retrieval applications, τ validation represents an insurmountable task.

Compared with τ , validation of VWC (and hence the underlying retrieval approach presented here) represents a much more accessible effort. VWC is primarily a mass-per-area quantity in kg/m^2 ; therefore, it can be measured more simply and directly with gravimetric methods. Since VWC represents the wet biomass of above ground vegetation, it plays a significant role in furthering our understanding of the variability of the carbon cycle and its dynamic interaction with the water and energy cycles.

In this paper, we propose a time series approach to using the tau-omega (τ - ω) model to retrieve vegetation water content (kg/m^2) directly with minimal use of ancillary data. Results from Monte Carlo simulations will be presented to establish the feasibility and robustness of this approach, followed by its application to one year (2016) of SMAP T_B observations.

2. FORMULATION

In passive microwave remote sensing of soil moisture, the tau-omega (τ - ω) model has often been used for soil moisture estimation. A common formulation of the model for T_B observed at an angle of θ can be found, for example, in [3]:

$$T_{Bp} = T_s e_p \exp(-\tau_p \sec \theta) + T_c (1 - \omega_p) [1 - \exp(-\tau_p \sec \theta)] [1 + r_p \exp(-\tau_p \sec \theta)] \quad (1)$$

where

$$r_p = r_{op} \exp(-h_p \cos^2 \theta) \quad (2)$$

In Eq. (1), the subscript p refers to either the horizontal or vertical polarization, T_s is the effective soil temperature, T_c is the vegetation canopy temperature (often assumed to be the same as T_s during the dawn hours for satellite morning overpasses), τ_p is the nadir vegetation opacity, ω_p is the vegetation single scattering albedo, and $r_p = 1 - e_p$ is the rough surface soil reflectivity, which is related to the smooth surface

soil reflectivity r_{op} according to Eq. 2 through the roughness coefficient h_p in an exponential term. In SMAP, Eqs. 1 and 2 allow soil moisture estimates to be inverted from T_{Bp} (from observations), T_s and τ_p (from ancillary data), as well as h_p and ω_p (from lookup table) through a soil dielectric model.

At L-band frequencies, ω_p (or the vegetation scattering mechanism that it represents) is often assumed to be small. With $\omega_p = 0$, Eq. 1 can be simplified as:

$$T_{Bp} = T_s [1 - r_{op} \exp(-\tau_{eff p})] \quad (3)$$

where

$$\tau_{eff p} = H_p + 2\tau_p \sec \theta \quad (4)$$

and

$$H_p = h_p \cos^2 \theta \quad (5)$$

Eq. 3 introduces the effective vegetation opacity ($\tau_{eff p}$). As seen from Eqs. 4 and 5, $\tau_{eff p}$ incorporates the combined radiometric and polarization effects of surface roughness (h_p) and vegetation opacity (τ_p). Despite its simpler form compared with Eq. 1, Eq. 3 is still primarily a function of soil moisture and effective vegetation opacity. As $\tau_{eff p}$ exhibits polarization dependence, there are $N + 2$ unknowns (N soil moisture estimates plus $\tau_{eff h}$ and $\tau_{eff v}$) for every N pairs of co-located T_{Bh} and T_{Bv} observations, assuming invariance of $\tau_{eff h}$ and $\tau_{eff v}$ during these T_B observations. To solve for these unknowns, $2N \geq N + 2$, or $N \geq 2$ pairs of T_{Bh} and T_{Bv} observations are required. Following this scheme, one year (2016) of SMAP T_B observations were used to produce time series snapshots of $\tau_{eff h}$ and $\tau_{eff v}$ whose annual means are shown in Fig. 1.

Substituting $\tau_p = b_p$ VWC in Eq. 4, one obtains the following relationships that relate the effective vegetation opacity to a scaled-and-shifted transformation of VWC:

$$\tau_{eff h} = H_h + 2 b_h VWC / \cos \theta \quad (6)$$

$$\tau_{eff v} = H_v + 2 b_v VWC / \cos \theta \quad (7)$$

In Eqs. 6–7, b_h and b_v are the polarization-dependent versions of the ‘ b ’ parameter commonly reported in the literature on passive microwave remote sensing of soil moisture [1–2]. In general, the ‘ b ’ parameter varies with microwave frequency, vegetation types, and polarization. As evident from Eqs. 6 and 7, there are $N + 4$ unknowns (N VWC estimates plus H_h , H_v , b_h , and b_v) for every N pairs of co-located $\tau_{eff h}$ and $\tau_{eff v}$ retrievals, assuming invariance of H_h , H_v , b_h , and b_v during these retrievals. In this study, the invariance of these parameters extends over the entire annual cycle of 2016.

In principle, it would take $2N \geq N + 4$, or $N \geq 4$ pairs of $\tau_{eff h}$ and $\tau_{eff v}$ retrievals from Eqs. 6 and 7 to retrieve VWC and the four polarization-dependent parameters in $[H_h H_v b_h b_v]$.

However, Eqs. 6 and 7 pose a unique challenge: certain unknowns (H_h and H_v) are additively combined with other unknowns (VWC, b_h , and b_v) to produce the retrieved $\tau_{eff h}$ and $\tau_{eff v}$. These two groups of unknowns can offset each other in many different ways for any given values of $\tau_{eff h}$ and $\tau_{eff v}$.

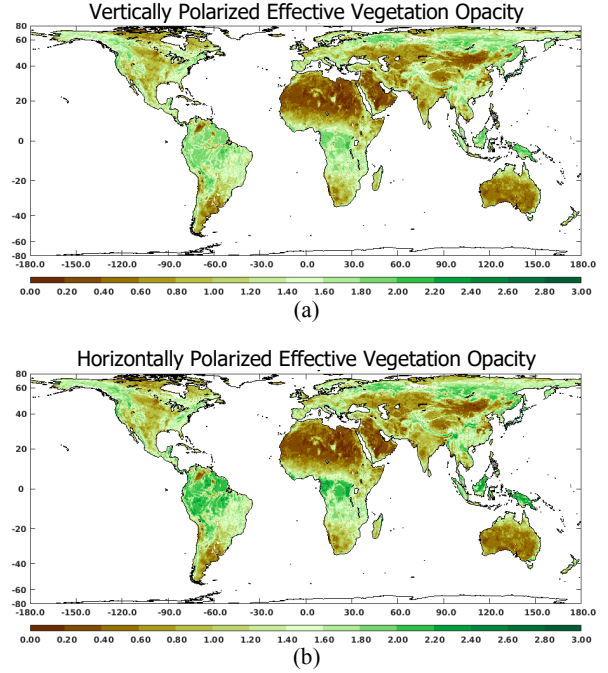


Fig. 1: Annual means of (a) vertically polarized effective vegetation opacity ($\tau_{eff v}$) and (b) horizontally polarized effective vegetation opacity ($\tau_{eff h}$) derived from one year (2016) of SMAP T_B observations.

The solution to Eqs. 6 and 7 is not unique, but it does not take on arbitrary values due to the temporal constraints of $\tau_{eff h}$ and $\tau_{eff v}$ on VWC. Using superscripts ‘T’ and ‘R’ to denote respectively the truth and retrieved parameters, it is evident that any VWC^R as a linear transformation of VWC^T in the form of $VWC^R = \alpha VWC^T + \beta$ is also a solution to Eqs. 6 and 7. Substituting $VWC^R = \alpha VWC^T + \beta$ into Eqs. 6 and 7, and equating the truth and retrieved parameters, one obtains the following relationships for $\alpha \neq 0$:

$$VWC^T = (VWC^R - \beta) / \alpha \quad (8)$$

$$b_v^T = \alpha \cdot b_v^R \quad (9)$$

$$b_h^T = \alpha \cdot b_h^R \quad (10)$$

$$H_h^T = H_h^R + 2 \cdot \beta \cdot b_h^R / \cos \theta \quad (11)$$

$$H_v^T = H_v^R + 2 \cdot \beta \cdot b_v^R / \cos \theta \quad (12)$$

3. SYNTHETIC DATA

To confirm the validity of these relationships between the truth and retrieved parameters, a Monte Carlo simulation experiment was set up, in which random vectors of $[VWC H_h H_v b_h b_v]$ were generated as inputs to Eqs. 6 and 7 to populate the truth $\tau_{eff h}$ and $\tau_{eff v}$ time series for 20 sample realizations. Nonlinear optimization subroutines were then invoked in each realization to search for the corresponding solution in the absence of perturbation noise. Figure 2(a) shows that for all sample realizations, VWC^R is indeed a linear transformation of VWC^T (with the 1:1 line in magenta), with gain (α) and offset (β) determined primarily by the values of the initial search vector elements. When the values of α and β determined from Fig. 2(a) were applied to Eqs. 9–12, the truth vector elements $[H_h H_v b_h b_v]$ were all perfectly reconstructed, as shown in Figs. 2(b)–(e).

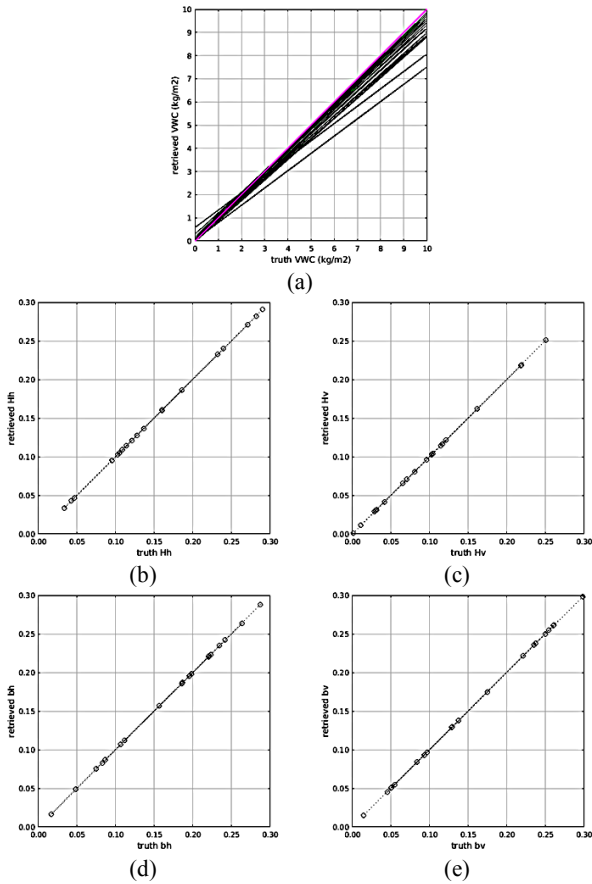


Fig. 2: (a) Eqs. 6–7 result in many solutions but each solution is a linear transformation of the truth, (b)–(e) confirm perfect reconstruction of H_h , H_v , b_h , and b_v according to Eqs. 9–12.

The robustness of this approach in the presence of perturbation noise can be evaluated using the same Monte Carlo simulation setup. Figure 3 shows the impacts of multiplicative uncertainties of various magnitudes (5%, 10%, and 20%) independently introduced to $\tau_{eff h}$ and $\tau_{eff v}$ on the inversion of VWC^T after the application of α and β . For

uncertainties as high as 20% (red line), the worst-case RMSE peaks at ~ 1.50 kg/m² up to a VWC^T level ~ 10.0 kg/m². As expected, retrieval error increases with increasing magnitude of uncertainty and VWC level.

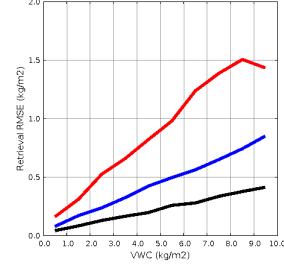


Fig. 3: Inversion of VWC out of 5,000 realizations from Eqs. 6–7 in the presence of uncertainties on $\tau_{eff h}$ and $\tau_{eff v}$. As uncertainty (5% [black], 10% [blue], and 20% [red]) and VWC level go up, retrieval error also goes up.

Despite the promising results of these Monte Carlo simulation results, it is important to observe what may *not* be applicable when dealing with real satellite data. First, random input vectors $[VWC H_h H_v b_h b_v]$ and the associated output vectors $[\tau_{eff h} \tau_{eff v}]$ were produced without any regard of their expected values at the frequency of interest (1.41 GHz in this study). In practice, this neglect would conceal any potential inconsistency between inputs and outputs that may still be present in the forward modeling of actual satellite T_B observations in the form of errors in T_B observations (e.g. NEAT) and ancillary data (e.g. effective soil temperature, soil texture). Such inconsistency could lead to retrieval of non-physical $[VWC H_h H_v b_h b_v]$.

Second, the success of this approach depends to a large extent the accuracy of α and β that convert VWC^R into VWC^T according to Eq. 8. In typical satellite applications of this retrieval approach where VWC^T is not available, α and β cannot be inferred as simply as illustrated in Fig. 2(a). Instead, they must be determined by external means. To this end, annual minimum and annual maximum from a climatological VWC database as used in SMAP [4] can be used as two reference points to estimate α (gain) and β (offset). To do so, one year of T_B observations can be used to derive $\tau_{eff h}$ and $\tau_{eff v}$ according to Eqs. 3–5. The resulting $\tau_{eff h}$ and $\tau_{eff v}$ can then be used in Eqs. 6–7 to construct an annual time series of VWC^R . Because $VWC^R = \alpha VWC^T + \beta$, a maximum (or minimum) VWC^R would correspond to a maximum (or minimum) of the climatological VWC (used as a surrogate of VWC^T) for $\alpha > 0$. This process can be repeated over all land pixels to map out α and β to reconstruct VWC^T from VWC^R .

4. REAL DATA

Using the global estimation procedure for α and β proposed above, one year (2016) of SMAP dual-channel T_B observations were used as inputs to the optimization processes in Eqs. 3–7. Figure 4 shows the corresponding

annual mean of VWC retrieval. The result indicates the expected geographical distribution of vegetation [5].

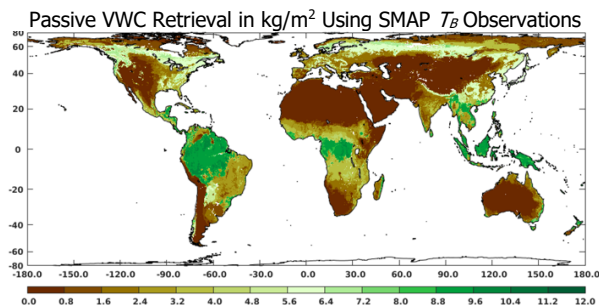


Fig. 4: Annual mean VWC retrieval using SMAP polarized T_B observations.

5. DISCUSSION

The tau-omega (τ - ω) model has been demonstrated in this paper to have a novel potential in VWC retrieval using polarized T_B observations. Preliminary results indicate that it is possible to make use of the difference in temporal scales between vegetation and surface roughness to retrieve VWC to within a gain factor α and an offset factor β , whose values can be inferred from external ancillary data. This work addresses a common validation challenge encountered in previous studies [6] on retrieval of vegetation opacity in nepers/m instead of VWC in kg/m^2 itself. Direct retrieval of VWC would improve our knowledge of the state of global forest biomass and its impacts on the carbon cycle. Following the confirmation from Monte Carlo simulations on the feasibility (Fig. 2) and robustness (Fig. 3) of this retrieval approach, real SMAP T_B observations were then used as a proof-of-concept experiment to produce a global estimate of VWC of expected geographical distribution of vegetation (Fig. 4).

6. CONCLUSION

A time series optimization approach was presented in this paper as a means to retrieve VWC in kg/m^2 using passive microwave observations from SMAP. Preliminary results support the analytical feasibility of this approach and its applicability to real data. Further time series validation analyses are needed to better quantify the retrieval accuracy against available *in situ* VWC ground truth. Alternate means to determine α and β are also desirable steps towards reducing dependence on external ancillary data. Finally, the impacts when ω_p is not negligible are also of interest for potential applications with T_B observations of higher frequencies.

7. ACKNOWLEDMENT

This part of the work carried out at the Jet Propulsion Laboratory was performed under a contract of California

Institute of Technology with the National Aeronautics and Space Administration.

8. REFERENCES

- [1] Jackson, T. J., 1993. *Measuring surface soil moisture using passive microwave remote sensing*, Hydrol. Process., vol. 7, pp. 139–152.
- [2] O’Neill, P. E., E. G. Njoku, T. Jackson, S. K. Chan, and R. Bindlish, 2015. *SMAP Algorithm Theoretical Basis Document: Level 2 & 3 Soil Moisture (Passive) Data Products*, Jet Propulsion Laboratory, California Institute of Technology, Pasadena, CA, JPL D-66480. https://nsidc.org/sites/nsidc.org/files/technical-references/L2_SM_P_ATBD_rev_D_Jun2018_auto_TOC.pdf (accessed: January 7, 2019).
- [3] Mo, T., B. J. Choudhury, T. J. Schmugge, J. R. Wang, and T. J. Jackson, 1982. *A model for microwave emission from vegetation-covered fields*, J. Geophys. Res., vol. 87, no. C13, pp. 11229–11237.
- [4] Chan, S. K., R. Bindlish, P. O’Neill, E. Njoku, T. Jackson, A. Colliander, F. Chen, M. Burgin, S. Dunbar, J. Piepmeier, S. Yueh, D. Entekhabi, M. H. Cosh, T. Caldwell, J. Walker, X. Wu, A. Berg, T. Rowlandson, A. Pacheco, H. McNairn, M. Thibeault, J. Martinez-Fernandez, A. Gonzalez-Zamora, M. Seyfried, D. Bosch, P. Starks, D. Goodrich, J. Prueger, M. Palecki, E. E. Small, M. Zreda, J. Calvet, W. T. Crow, Y. Kerr, 2016. *Assessment of the SMAP passive soil moisture product*. IEEE Trans. Geosci. Remote Sens. 54 (8), 4994–5007.
- [5] Chan, S. K., R. Bindlish, R. Hunt, T. Jackson, and J. Kimball, *SMAP ancillary data report on vegetation water content*. Jet Propulsion Laboratory, California Institute of Technology, Pasadena, CA, JPL D-53061, http://smap.jpl.nasa.gov/system/internal_resources/details/original/289_047_veg_water.pdf (accessed: January 7, 2019).
- [6] Konings, A. G., M. Piles, K. Roetzer, K. A. McColl, S. Chan, and D. Entekhabi, 2016. *Vegetation optical depth and scattering albedo retrieval using time series of dual-polarized L-band radiometer observations*, Remote Sensing of Environment, Volume 172, Pages 178-189.